ELSEVIER

Earth and Planetary Science Letters 148 (1997) 501–516

EPSL

Mantle-derived helium and carbon in groundwaters and gases of Mount Etna, Italy

Patrick Allard [a,*], Philippe Jean-Baptiste [b], Walter D'Alessandro [c], Francesco Parello [d], Bianca Parisi [d], Christine Flehoc [b]

[a] *Centre des Faibles Radioactivités, CNRS-CEA, Orme de Merisiers, 91191 Gif sur Yvette Cedex, France*

[b] *Laboratoire de Modélisation du Climat et de l'Environnement, CEA / DSM, Orme des Merisiers, 91191 Gif sur Yvette Cedex, France*

[c] *Istituto di Geochimica dei Fluidi, CNR, 90133 Palermo, Italy*

[d] *Istituto di Mineralogia, Petrografia e Geochimica, Università di Palermo, 90133 Palermo, Italy*

Received 18 October 1996; revised 25 February 1997; accepted 2 March 1997

Abstract

We report the first detailed investigation of both helium and carbon isotopes in groundwaters and gases of Mt. Etna, providing new insight into the distribution, origin and budget of magmatic gas release at this very active volcano [1]. A mantle-derived magmatic component, with ultimate $^3He/^4He$ ratio of 6.9 ± 0.2 R_a and $\delta^{13}C$ of about $-4‰$, is identified in both types of fluids, depending on their location and the extent of their dilution by either air (gases) or a mixture of dissolved air and organic carbon (waters). Apart from the summit zone, this magmatic component is preferentially concentrated in CO_2-rich groundwaters that issue from two remote sectors of the south-southwest and eastern volcano flanks, where its proportion increases with the altitude of meteoric recharge (or the length of pathflow) of the waters. Such a pattern suggests that, in addition to possible local gas input, the groundwaters collect much of their dissolved magmatic He and C while they infiltrate and flow through one of the more elevated, gas-effusing parts of the volcanic pile, among which the south-southeast fracture zone of Etna is the best candidate. These observations provide a new framework for remote geochemical monitoring of the volcano.

The $^3He/^4He$ ratio of the magmatic gas end-member coincides with that of helium trapped in the He-rich olivine crystals of Etna basalts (mean range: 6.7 ± 0.4 R_a, [2,3]), pointing to its negligible dilution by radiogenic He from the crustal basement and further constraining the $^3He/^4He$ ratio of the present-day Etna magma. While being lower than the typical MORB value of 8 R_a, this ratio is the highest for an active volcano in continental Europe and probably tracks a relatively radiogenic upper mantle zone that is upwelling beneath this region [4]. The estimated outputs of mantle-derived CO_2 and ^3He from Etna account for 10% and 15%, respectively, of estimates for global subaerial volcanic emissions. This huge contribution results from continuous degassing of mostly unerupted He- and C-rich alkaline basaltic magma, which occurs principally through the central open conduits and secondarily through the flanks of the volcano. Groundwaters carry only a minor fraction ($\approx 3\%$) of total emitted CO_2 and ^3He.

Keywords: Mount Etna; helium; carbon; gases; groundwaters; isotopes; mantle; magma degassing

* Corresponding author: Tel.: +33 169088542. Fax: +33 169087716. E-mail: allard@obelix.saclay.cea.fr

PII S0012-821X(97)00052-6

1. Introduction

Mount Etna, the largest active volcano in Europe (40 km wide, 3.3 km high a.s.l.), is unique among terrestrial volcanoes for both its peculiar geodynamic setting and huge volatile discharge. Built over the last 200 kyr in eastern Sicily, along tensional faults cutting a $\geq$ 16 km thick continental crust [5], Etna is erupting alkali basalts–hawaiites at the collision boundary of two continental plates (Africa and Eurasia) [6] and in front of an active subduction zone (Aeolian island arc; Fig. 1). While sharing compositional affinities with intra-plate oceanic basalts [5–7], its lavas display geochemical singularities, such as a high volatile content [8–10] and moderate subduction-like anomalies (relatively high U–Th/K, Th/Ta and La/Tb ratios; e.g. [6,11,12]), which suggest a complex mantle source. A voluminous summit crater plume, as well as diffuse flank emanations, continuously escape from the volcano, resulting in the greatest known permanent contribution of volcanic volatiles to the atmosphere [1]. The magmatic origin of this huge gas release has been verified from stable isotope analysis of water, sulphur and carbon in the high temperature crater exhalations [13,14] and of carbon in soil emanations [1], although a possible addition of CO_2, derived from heated carbonate sequences in the basement, was considered in the case of more distal emanations, richer in ^{13}C [1].

Additional constraints upon the source of Etnean volatiles (and lavas) can be obtained from the isotopic ratio of helium which, due to its contrasting values in the continental crust (≤ 0.1 R_a) and in the upper (8 ± 1 R_a) and lower (≥ 35 R_a) mantle (R_a being the atmospheric ratio of 1.38×10^{-6}), is a powerful tracer of the origin (e.g., [15]) and possible crustal dilution [16–18] of mantle-derived fluids. The first He isotopic determination at Etna [1] indicated a minimal $^3He/^4He$ ratio of 5.0 R_a in air-diluted soil gas from the summit area, with a largely uncertain corrected value of ≈ 8 R_a. More recent analyses of helium trapped in olivine crystals of both

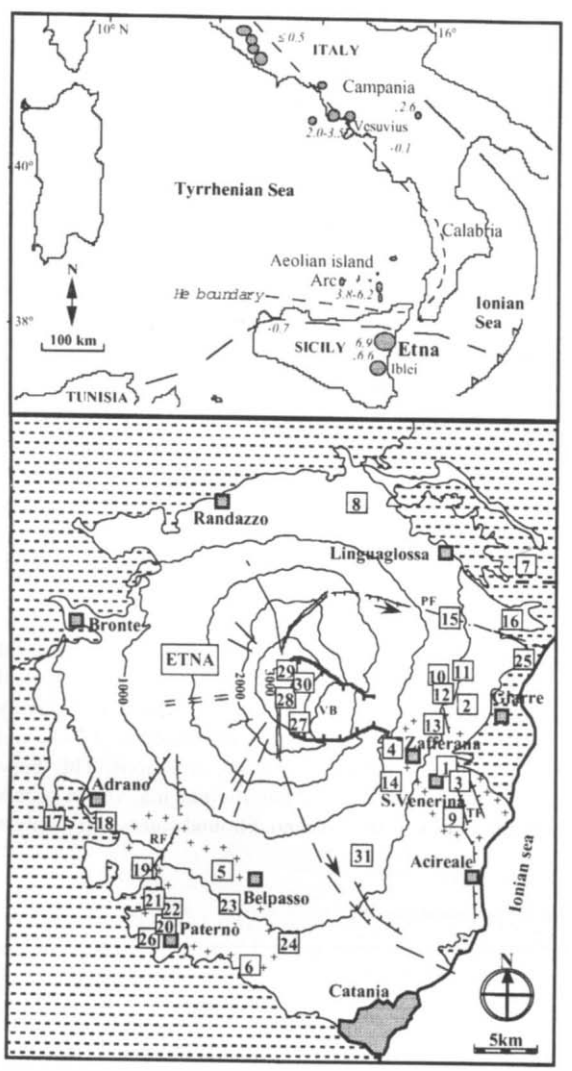

Fig. 1. Tectonic setting of Etna and location of water and gas sampling sites. Upper map shows Quaternary/active volcanic sites (dark areas) in Central–Southern Italy and R/R_a ratios (in italics) in related volcanic fluids [42–45], together with the proposed [42] 'helium boundary' (short dashed line) with high ratios inside the line and low ratios outside. The long dashed line approximates the collision boundary between the African and European continental plates [5]. The solid line marks the external front of the Metaponto and Gela belt. Lower map: water and gas sampling sites on Etna are numbered as in Table 1 and 2. Highest R/R_a ratios in groundwaters (Table 1) are found in two sectors of the south-southwest (Belpasso–Paterno) and eastern (Zafferana) volcano slopes (delimited with crosses), where the highest CO_2 concentrations in soils and waters also occur ([23] and this work). Volcanotectonic structures [39] include summit rift zones (=), eruptive fissure swarms (dashed lines), the Valle del Bove depression (*VB*) and main seismogenic faults (*RF* = Ragalna fault; *TF* = Timpe fault; *PF* = Pernicana fault). Relative displacements along faults bordering the southeastern Etna block are shown by arrows. Dashed areas = sedimentary rocks; stippled areas = towns.

ancient and recent Etna basalts [2,3] have yielded $^3He/^4He$ ratios ranging from 4.9 to 8.2 R_a, with a mean of 6.7 ± 0.4 R_a [2,3], which suggest a source with lower $^3He/^4He$ ratio than typical MORB-type upper mantle and exclude the hypothesis of a ^3He-rich hot spot [2–4].

Here we provide new data about the origin, distribution and budget of magmatic gas leaks at Etna, based on a detailed isotopic study of both helium and carbon (plus H and O) in groundwaters and gases from the volcano. In particular, we report the first He isotope data set on Etnean groundwaters, the study of which was stimulated by the idea that they should carry both a space- and time-integrated imprint of the inputs of magmatic gas [16]. Our results complement the genetic information gathered from the lava samples but also provide further insight into the interactions between magma degassing and the hydrological system of the volcano, opening new perspectives for its remote geochemical monitoring.

2. Measurements

A series of water springs, water wells and gas emanations (fumaroles, mofettes, CH_4-rich gas and bubbles in water) were sampled in different sectors of the volcano (Fig. 1) and were analyzed for both their chemistry and isotopic composition. The results are reported in Tables 1 and 2. The temperature, pH and conductivity of groundwaters were measured in the field and their alkalinity determined by immediate titration. For He isotope analysis, waters were sampled in copper tubes from which the dissolved helium was subsequently extracted under vacuum, following a routine procedure [19]. Gases were collected in vacuum glass containers with stopcocks and analyzed directly. Chemical analysis of waters and gases, as well as isotopic analysis of dissolved and gaseous carbon ($\delta^{13}C \pm 0.1‰$, versus PDB standard), were done at IMPG (Palermo University), as already described [20]. The D/H ratios ($\delta D \pm 0.5‰$) and $^{18}O/^{16}O$ ratios ($\delta^{18}O \pm 0.09‰$) of waters, referred to SMOW standard, were determined in LMCE (CEA, Saclay) with MAT-252 and LODO mass spectrometers, respectively. He isotope measurements were made in the same laboratory with a VG-3000 mass spectrometer operated in routine for oceanic helium samples [19] and connected with a high-vacuum inlet line ensuring a low helium blank ($< 6 \times 10^{-10}$ cm^3 STP). The accuracy on reported helium contents is better than 0.8% and the analytical uncertainty on $^3He/^4He$ ratios, calibrated against an atmospheric standard, is about 1%. He was not separated from Ne, which may introduce a significant bias in a measured $^3He/^4He$ ratio when the Ne/He ratio is quite a bit higher than that of the standard [21,22], depending on the actual pressure in the source of the mass spectrometer [22]. However, this effect was verified [19] to be minimal when analyzing samples with a neon concentration similar to or lower than that in air-saturated water or air, which is typically the case of air-diluted groundwaters and hydrothermal fluids analyzed in this study.

3. Results

3.1. Origin and chemistry of groundwaters

A purely meteoric origin for all analyzed waters is demonstrated by their δD (-51.5 to $-29.1‰$) and $\delta^{18}O$ (-8.7 to $-6.1‰$), which define a linear relationship ($\delta D \approx 8\delta^{18}O + 19$; Fig. 2) typical of

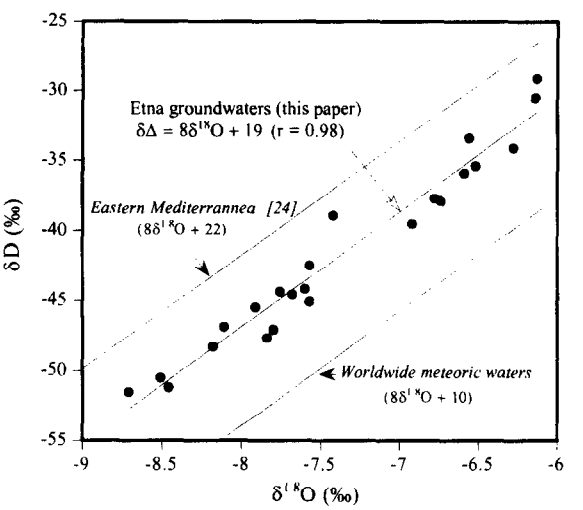

Fig. 2. δD–$\delta^{18}O$ relationship in analyzed groundwaters. The data define a linear trend of mean value $\delta D = 8\delta^{18}O + 19$, typical of precipitations in the Etna region [23] and Central Mediterranean [24], which evidences a purely meteoric origin for all waters analyzed. Also drawn are the lines for meteoric waters worldwide and in the eastern Mediterranean [24].

Table 1
Chemical and isotopic abundances of helium and carbon in the groundwaters of Mt. Etna

Sampling sites	Elevation (m)	T (°C)	pH	Conductivity (μS/cm)	HCO_3^- (mol/l 10^{-3})	TDC (mol/l 10^{-3})	pCO_2 (atm)	Mg^{2+} [a] (mol/l 10^{-3})	δD (‰ ± 0.5)	$\delta^{18}O$ (‰ ± 0.09)	^4He (cm^3/g 10^{-8})	$^3He/^4He$ (R/R_a)	$\delta^{13}C$ TDC (‰ ± 0.1)	$\delta^{13}C$ CO_2 (‰ ± 0.1)	Δh (m)
1 San Venerina galleria (s)	250	20.6	6.77	1677	14.0	19.8	0.174	°7.11	−44.6	−7.68	5.16	1.73	−0.2	−5.9	1017
2 San Venerina sorgente (s)	270	20.4	6.80	1607					−44.2	−7.60	4.92	1.74			900
3 San Paolo (w) 10/93	325	16.6	6.78	876	7.9	11.1	0.102	°3.23	−35.9	−6.59	9.03	3.12	−2.8	−8.7	838
3 San Paolo (w) 09/94	325	17.6	6.59	922	8.2	13.5	0.175	3.29			9.97	3.03	−3.3	−8.1	838
3 San Paolo (w) 03/95	325	15.6	6.71	1120	8.6	13.4	0.154	3.39			10.33	3.09	−3.8	−8.6	838
3 San Paolo (w) 04/95	325	16.4	6.97	905	8.4	12.5	0.127	3.72			13.14	3.19	−2.8	−8.4	838
4 Piano dell'Acqua (s)	738	14.8	7.85	214	2.3	2.4	0.003	°0.71	−33.4	−6.56	3.77	1.00	−0.3	−8.4	115
5 Acqua Difesa (w) 10/93	600	16.2	6.29	1090	13.7	31.2	0.551	6.90	−45.1	−7.57	19.30	5.52	−1.4	−3.8	912
5 Acqua Difesa (w) 08/94	600	20.5	6.06	1217	15.1	47.2	0.971	6.63			51.17	6.29	−1.0	−3.9	912
5 Acqua Difesa (w) 09/94	600	16.8	6.18	1212	14.4	38.4	0.740	6.90			32.72	6.39	−1.1	−3.7	912
5 Acqua Difesa (w) 10/94	600	16.4	6.07	1092	13.6	42.5	0.906	7.04			60.30	6.48	−1.7	−3.7	912
5 Acqua Difesa (w) 03/95	600	14.8	6.18	894	12.9	34.4	0.676	6.12			34.42	6.25	−1.5	−3.9	912
6 Pozzo Cuscuna (w)	309	13.8	7.10	1250	14.9	17.9	0.071	9.02	−39.5	−6.92	5.20	1.48	−1.0	−8.5	734
7 Taormina (s)	75	18.4	7.50	988	8.2	8.3					4.75	1.00			
8 Azienda Cambria (w)	570	10.5	7.02	587	6.0	7.5	0.052		−48.3	−8.18	5.41	2.27	−6.0	−13.4	823
9 Pozzo Guardia (w) 10/93	250	15.3	6.40	686	6.9	13.6	0.219	3.14	−34.1	−6.28	5.04	2.61	−2.2	−6.1	770
9 Pozzo Guardia (w) 10/94	250	15.7	6.24	716	6.6	16.0	0.300	2.94			6.30	3.06	−3.5	−6.5	770
9 Pozzo Guardia (w) 03/95	250	15.3	6.26	698	7.0	16.7	0.318	3.22			6.37	2.90	−3.1	−6.1	770
10 Sorgente Fornazzo (s)	825	14.2	8.10	205	1.5	1.5	0.001	°0.32	−29.1	−6.13	4.75	1.01	−13.0	−22.0	0
11 Cento Cavalli (s)	700	13.8	8.40	320	1.5	1.5	0.001	°0.84	−37.7	−6.78	7.47	1.60	−11.8	−20.9	210
12 Sorgente Nunziata (s)	250	13.5	8.20	480	3.1	3.1	0.002	°2.47	−35.4	−6.52	6.63	1.38	−10.3	−19.4	590
13 Pozzo Primoti (w) 10/93	525	21.2	6.51	2120	14.8	24.2	0.272	8.49	−45.5	−7.91	4.76	3.04	−1.0	−4.9	915
13 Pozzo Primoti (w) 10/94	525	21.5	6.32	1840	15.1	33.3	0.527	6.93			5.10	3.15	−1.1	−4.2	915
13 Pozzo Primoti (w) 01/95	525	21.0	6.26	1920	15.5	37.0	0.635	7.13			5.80	3.49	−1.3	−4.1	915
13 Pozzo Primoti (w) 04/95	525	21.0	6.77	1770	15.2	21.7	0.192	8.08			5.04	3.32	−1.6	−6.9	915

14 Pozzo Ilice (w) 10/93	780	9.3	6.46	193	2.7	3.8	0.038	0.84	−38.9	−7.42	5.28	1.63	−4.5	−9.0	550
14 Pozzo Ilice (w) 10/94	780	10.1	6.52	217	3.8	6.7	0.100	0.66			5.36	1.61	−4.4	−9.3	550
15 Sorgente Vena (s)	720	12.7	7.80	235	1.3	1.4	0.002	°0.91	−30.5	−6.14	68.60	4.57	−12.5	−21.5	0
16 Pozzo Piedimonte (w)	375	13.5	7.70	544	4.3	4.5	0.007	°1.87	−44.4	−7.76	12.20	1.00	−7.7	−16.4	875
17 Pozzo Adrano (w)	200	16.7	7.41	1797	14.2	15.7	0.044		−47.7	−7.84	3.95	1.20	−3.2	−11.2	1080
18 Sorgente Adrano (s)	400	15.7	8.30	2050	14.0	14.2	0.006	10.20	−47.1	−7.80	4.71	1.00	−6.2	−15.0	890
19 S. Maria Licodia (s) 07/93	390	14.6	6.99	953	11.9	15.0	0.098				4.60	1.47	−0.4	−7.4	1113
19 S. Maria Licodia (s) 10/93	390	15.8	6.89	978	11.7	15.5	0.119	7.13	−50.5	−8.51	5.77	1.71	−0.9	−7.4	1113
19 S. Maria Licodia (s) 11/94	390	14.8	6.94	980	12.3	15.8	0.112	6.28			5.41	1.59	−1.3	−7.9	1113
20 Acqua Grassa (s) 07/93	210	19.8	6.15	2240	23.3	64.3	1.230				26.00	5.80	−1.5	−3.9	1160
20 Acqua Grassa (s) 10/93	210	19.8	6.12	1861	23.1	66.6	1.306	11.74	−46.9	−8.11	12.60	5.63	−1.2	−4.1	1160
20 Acqua Grassa (s) 06/94	210	19.4	6.16	2036	23.4	63.6	1.213	11.43			11.84	5.91	−1.1	−3.8	1160
20 Acqua Grassa (s) 03/95	210	19.1	6.15	1898	23.6	65.7	1.278	10.71			7.06	5.78	−1.6	−3.9	1160
21 Romito Blu (s)	323	14.2	6.79	1383	15.8	22.2	0.207		−51.5	−8.71	13.80	3.69	−0.8	−6.9	1247
22 Romito Rossa (s) 03/94	318	15.3	6.60	1473	16.3	26.6	0.326	8.94	−51.2	−8.46	77.90	4.56	−1.7	−6.8	1169
22 Romito Rossa (s) 09/94	318	15.4	6.88	1258	16.1	21.4	0.169	7.68			60.50	4.42	−1.6	−8.1	1169
22 Romito Rossa (s) 03/95	318	14.6	6.95	2086	16.4	21.0	0.146	8.52			55.23	4.47	−2.6	−8.6	1169
23 Acquarossa (w) 10/93	340	18.4	6.70	1815	24.2	58.2	1.040	13.16	−42.5	−7.57	36.10	6.23	−1.2	−4.1	850
23 Acquarossa (w) 09/94	340	24.4	6.23	1826	24.7	61.6	1.024	18.14			25.44	6.36	−1.2	−3.8	850
23 Acquarossa (w) 04/95	340	21.1	6.71	1880	27.8	41.7	0.408	15.19			32.01	6.00	−0.7	−5.9	850
24 Pozzo San Leonardo (w)	460	16.2	6.90	1392	15.1	19.8	0.148	8.70	−37.9	−6.74	12.90	4.76	−1.8	−6.3	727
31 Pozzo Pedara (w) 05/94	730	14.8	7.81	327	2.9	3.0	0.003	1.30			20.82	4.92	−9.1	−17.8	
Air-saturated water [b]		20.0									4.52	0.99			

[a] Mg^{2+} values preceded by ° are from [23].

[b] From [29].

Sampling sites numbered as in Fig. 1. s = spring; w = well. When unspecified, the sampling date was October 1993. Total dissolved carbon (TDC) and pCO_2 values were computed from the measured temperature, alkalinity (HCO_3^-) and pH of each water. In the pH range observed here most dissolved carbon occurs as HCO_3^- and $CO_{2(aq)} \approx H_2CO_3$. δD and $\delta^{18}O$ values versus SMOW standard. $^4He/^4He$ ratios, expressed as R/R_a (where R_a is 1.38×10^{-6}), are not corrected for air dilution (see text). The $\delta^{13}C$ (versus PDB standard) of gaseous CO_2 in isotopic equilibrium with dissolved carbon at sampling temperatures was derived from the measured $\delta^{13}C$ of TDC and the relationship: $\delta^{13}C(CO_2) \approx \delta^{13}C(TDC) + \varepsilon(CO_2 - H_2CO_3) - x \cdot \varepsilon(HCO_3 - H_2CO_3)$, where $\varepsilon(X - Y)$ is the permil ^{13}C fractionation between corresponding carbon species (taken from data in [33]) and x is the HCO_3/TDC concentration ratio (see text). Δh is the difference (in meters) between the altitudes of meteoric recharge and outflow of the groundwaters, which provides a measure of the length of their pathflow (see text). Recharge altitudes were computed from the $\delta^{18}O$ of each water and the vertical ^{18}O gradient of 0.3‰ per 100 m for local precipitations [23].

Table 2
Isotopic composition of helium and carbon in gases of Etna.

Sampling site	Type	Altitude (m)	T (°C)	CO_2 (%)	CH_4 (%)	N_2 (%)	O_2 (%)	$\delta^{13}CO_2$ (‰ ± 0.1)	^4He (ppm)	$^3He/^4He$ (R/R_a) (±1%)	$CO_2/^3He$ (10^9)
20 Acqua Grassa [a]	gas bubbles	210	18.7	98.5	0.018	1.5	< 0.05	−4.4	14.7	5.63	8.6
23 Acquarossa [3]	gas bubbles	340							34	5.50	3.4
25 Fondachello	gas bubbles	8	19.3	0.6	93.1	6.3	< 0.1	−25.0	478	5.90	0.001
26 Paterno, Salinella 1	mud pool gas	250	19.1	94.1	4.2	1.3	0.4	−0.4	18.8	6.11	5.9
26 Paterno, Salinella 1	mud pool gas	250	19.1	94.2	4.2	1.3	0.4	−0.4	17.1	6.00	6.9
26 Paterno, Salinella 2	mud pool gas	240	19.5	94.7	3.1	1.7	0.6	−0.3	15.8	6.15	7.0
26 Paterno, Salinella 2	mud pool gas	240	19.5	94.6	3.1	1.6	0.6	−0.3	18.3	6.06	6.3
26 Paterno, Salinella [3]	mud pool gas	250							115	5.91	1.0
Paterno, mud volcano [3]	mud pool gas	220							63	6.34	1.6
27 1989 eruptive fissure	fumarole	2850	97.0	22.9	0.013	64.2	12.9	−1.1	3.8	1.59	27
28 Southeast crater [1]	soil gas	3080	81.0	8.1		74.2	17.7	−4.1	6.6	2.83	3.2(5.2)
29 Bocca Nuova crater [1]	soil gas	3240	61.0	27.9		57.9	14.2	−3.7	9.3	5.00	4.3(5.3)
30 Voragine crater rim	fumarole	3300	135	0.1	0.29	86.0	19.6		3.1	1.23	0.2
Etna magmatic gas [b]			1090	86.7	0	2.8	0.7	−4.0 ± 0.5	15.8	6.9 ± 0.2	5.8
Atmosphere			25.0	0.036		78.1	20.9	−7.6	5.24	1.00	0.055

Included are previous data from [1] and [3], with $^3He/^4He$ ratios from [3] corrected for air dilution. The $\delta^{13}C$ range includes the result on this and other samples of Etna eruptive exhalations [13,14]. The R/R_a ratio is that of the magmatic end-member inferred in this paper (see text and Fig. 3). $CO_2/^3He$ ratio in brackets for samples 28 and 29 was corrected assuming all nitrogen to be atmospheric.

[a] He content and R/R_a ratio of the gas in equilibrium with dissolved helium in the water.

[b] Measured He and CO_2 contents of 1090°C gas from erupting NE summit crater in 09/1986 (P.A., unpubl. data; the values allow for the presence of additional species).

precipitations on the volcano [23] and in the Central Mediterranean [24]. The lack of any positive ^{18}O shift, which indicates no isotopic exchange with hot rocks, is consistent with previous isotopic data [23] and with hydrological evidence for both a rapid infiltration and transit of meteoric groundwaters forming on Etna [25–27]. These quickly infiltrate through the permeable/fractured volcanic layers, with minor loss by evapotranspiration, and then flow downward along the contact with the impermeable upper sedimentary basement (allochthonous flysch units which, to the WNW, rise over 1000 m a.s.l. [6,25]). This hydrogeological confinement explains why most groundwater run-off occurs on the lower volcano slopes, with quite a high flow rate (from a few hundred to a few thousand litres per second for the largest springs [25–27]). Estimates of the effective lateral velocity of representative aquifers, from 21 to 430 m/day [25–27], suggest groundwater residence times from half a year to a few years.

Despite their purely meteoric origin, many of the waters analyzed are highly enriched in bicarbonate and total dissolved carbon (TDC), as previously recognized by Anza et al. [23]. Their pCO_2 exceeds by one to three orders of magnitude the corresponding values in air ($10^{-3.6}$ atm) and standard soil (10^{-3} atm), reaching over 1 atm at a few sites where water is bubbling (Table 1). This, and the dominant proportion of CO_2 in the dissolved gaseous fraction [28], prove that the groundwaters interacted with a CO_2-rich gas phase. HCO_3^- is the dominant ionic species in solution and its variations perfectly match those of conductivity and total dissolved salt. Sulphate and chlorine are significant in only a few waters issuing along the eastern flank of the volcano (1, 3, 9 and 13; Fig. 1), where late Pliocene–Quaternary sediments outcrop [23,25]. Among the cations, Mg and Na commonly prevail over Ca and K, giving most waters a typical alkali earth–bicarbonate composition [23], consistent with their circulation through basaltic rocks and their broad isolation from limestones in the basement by the impermeable upper flysch units [25]. The positive correlation of HCO_3^- with the cation content (especially strong with magnesium, $r^2 = 0.93$) and its negative correlation with pH indicate that the compositional

range of most waters reflects the extent of their acid attack of the host basalts (gradual conversion of CO_2 into bicarbonate and rise in pH). This extent depends on both their initial CO_2 content (the inferred pCO_2 values correspond to initial CO_2 concentrations of 10^{-3} to 10^{-1} mol/l and initial pH values ≤ 4 [23]) and their residence time and/or the length of their pathflow. The latter was tentatively estimated from the difference (Δh, Table 1) between the altitude of formation of each water, determined from its $\delta^{18}O$ and the ^{18}O vertical gradient for local precipitations ($\approx 0.3‰$ per 100 m, [23]), and its altitude of outflow (corrected for depth in the case of wells). The low flanks of Etna have a mean slope of 5–10% [25]. The results (Fig. 5a,b) show that both HCO_3^- (or TDC) and Mg^{2+} do tend to increase with the water pathflow length, with a steeper rate for Δh values ≥ 800 m; that is, for higher recharge elevations. The implications of this trend are discussed in Section 3.4, together with the isotopic results for He and C.

3.2. He isotopes in groundwaters and gases

Most groundwaters analyzed are also enriched in ^4He and ^3He (by up to 17 and 80 times, respectively) with respect to air-saturated water at in situ temperature and conductivity [29]. Their measured (uncorrected) $^3He/^4He$ ratios range from 1.0 to 6.48 R_a (Table 1). Gas emanations display a similar $^3He/^4He$ range, from 1.6 to 6.34 R_a, when including the few data previously reported (Table 2). Such ratios evidence a contribution of ^3He-rich helium of mantle (magmatic) origin to both types of fluids. In the case of waters, minor ^3He addition is expected from tritium decay, given their short hydrological cycle; no tritium data is yet available but, even assuming that these would have formed 12 years ago (about one tritium decay period), from precipitations containing 20 TU [30], the accumulated amount of tritiogenic He (2.4×10^{-14} cm^3 STP/g H_2O) would contribute only 0.3% of the highest $^3He/^4He$ ratios and 20% of the lowest ones, whose the value and the corresponding dissolved He content are just atmospheric. Likewise, given the low abundance of lithium in Etna basalts (45–60 ppm, [31]), only negligible ^3He could be added from thermal neutron (n,α) reaction on ^6Li in the host rocks [32].

Plotting ^3He versus ^4He in both waters and gases (Fig. 3) allows us to constrain the ultimate $^3He/^4He$ ratio of the magmatic helium component and to assess its potential dilution by radiogenic helium (≤ 0.1 R_a, [32]) produced by U–Th decay in Etna's basement, the lower half of which is crystalline [5]. Three features are noteworthy:

1. Most groundwaters plot on a simple mixing trend between air-saturated water (ASW) and a magmatic end-member whose R/R_a ratio, as given by the slope of the line, is 6.9 ± 0.2. This component represents 90–94% of our samples (5 and 23) with the highest $^3He/^4He$ ratio. Soil gases from the summit crater zone plot on an air dilution trend of the same magmatic component.
2. The inferred R/R_a ratio of this latter coincides with the upper bound of the mean range (6.7 ± 0.4) reported for He trapped in olivine crystals of both ancient and recent Etna basalts [2,3] and, especially, with the R/R_a ratio of early crystallized He-richest olivines. Such a similarity implies a negligible contamination of the magmatic gas by crustal He from the basement and adds a further constraint to the $^3He/^4He$ signature of present-day Etna magma.
3. A contribution of crustal helium is significant to only a few groundwaters (15, 16, 21, 22 and 31) and a few gas manifestations (25 and 26, Table 2), all located at or near to the northeast and southwest periphery of the volcano (Fig. 1), whose points are shifted to the right of the 'magmatic' line. This crustal contribution is still clearer when normalizing ^3He and ^4He in groundwaters to TDC. Otherwise, there is no gradual trend of decreasing $^3He/^4He$ with distance from the central conduits, contrary to what has been observed at other volcanoes [16–18]. This enhances the idea of a broadly minor crustal dilution of the magmatic helium during its ascent and subsequent transport by groundwaters. Such a pattern provides very favourable conditions for a He isotopic survey of magmatic gas in the water discharges of Etna, whose the first results will be presented elsewhere.

3.3. He–C isotope relationships

Apart from the summit zone, where fumaroles and soil gases are strongly diluted by air ($^3He/^4He$

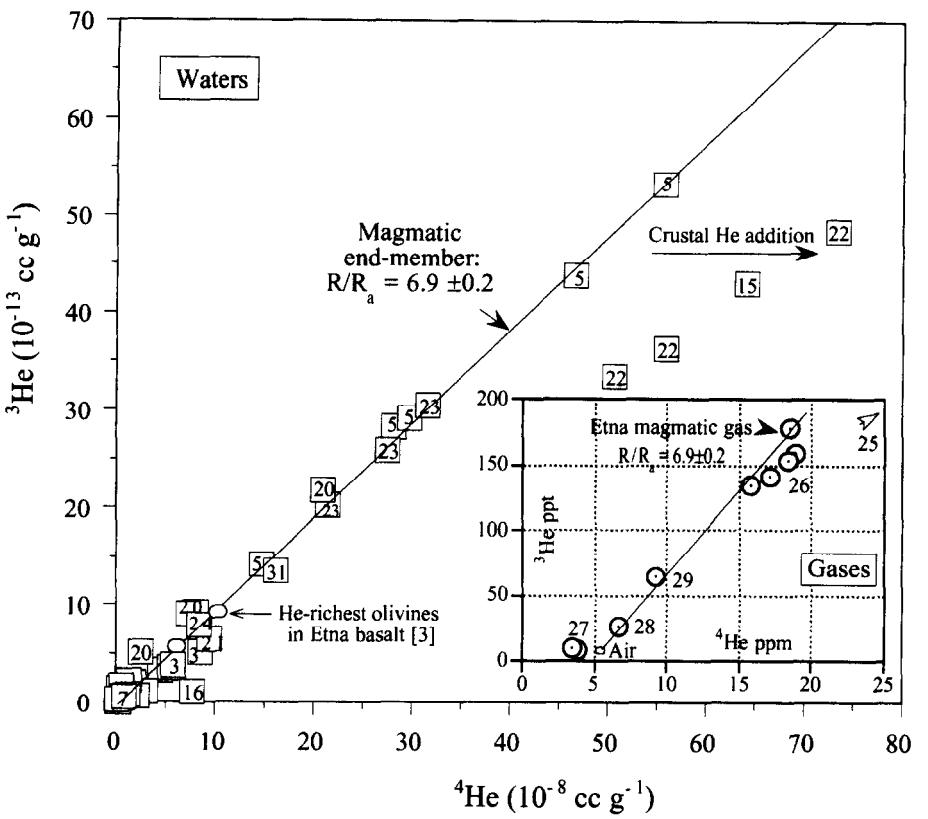

Fig. 3. ^{3}He versus ^{4}He in Etna groundwaters and gases. Reported ^{3}He and ^{4}He contents in groundwaters are those in excess of air-saturated concentration at the corresponding temperature and conductivity [29]. Note that most samples are simple binary mixtures of dissolved atmospheric He and a ^{3}He-rich magmatic component whose R/R_a ratio, as given by the slope of the line, is 6.9 ± 0.2. Soil gases from Etna summit zone plot along air dilution of the same component (inner diagram). The addition of crustal-derived ^{4}He is broadly negligible, except for a few waters (15, 16, 21, 22 and 31) and a few gas manifestations (24 and 25), located at or towards the southeast and west-northwest periphery of the volcano. The point for 'Etna magmatic gas' is derived from the He content of the high-temperature summit crater gas (15.8 ppm, Table 2) and the R/R_a ratio of 6.9 ± 0.2 inferred from the water samples.

≤ 5.0 R_a, Table 2), the spatial distribution of ^{3}He/^{4}He ratios reveals a preferential occurrence of the mantle-derived helium in groundwaters and gases that issue from two remote sectors of the southern (Belpasso–Paterno) and eastern (Zafferana–S. Venerina) volcano flanks (Fig. 1). As already recognized [23], groundwaters in these two areas—especially the southern one—display highest TDC and pCO_2 (Table 1). We find here a positive correlation between their carbon content and ^{3}He/^{4}He ratio (Fig. 4a), with some scattering being due in part to seasonal variations at a given site (5, 13, 20 and 23). This correlation suggests a common magmatic derivation of the dissolved He and C, which is confirmed by carbon isotopic data (Table 1). The measured $\delta^{13}C$ of TDC in these waters is remarkably constant, between −1.8 and −1.0‰, despite wide pCO_2 variation (Fig. 4b). The $\delta^{13}C$ of gaseous CO_2 in chemical and isotopic equilibrium with the dissolved carbon at the water temperature was computed from the relationship:

$$\delta^{13}C(CO_2) = \delta^{13}C(TDC) + \varepsilon(CO_2 - H_2CO_3) - x \cdot \varepsilon(HCO_3 - H_2CO_3)$$

where $\varepsilon(X - Y)$ is the permil ^{13}C fractionation between corresponding carbon species and x is the HCO_3/TDC concentration ratio (in the pH range observed here CO_3^{2-} is negligible, all carbon being

dissolved as bicarbonate and $CO_2(aq) \approx H_2CO_3$). Data in [33] lead to:

$$\delta^{13}C(CO_2) = \delta^{13}C(TDC) + 1.31 - 0.0049t°C - x(12.09 - 0.1189t°C)$$

A restricted $\delta^{13}C$ range from -4.5 to $-3.7‰$ (Table 1 and Fig. 4c) is obtained for the corresponding CO_2, presumably representative for the original gas. At a few sites where water is bubbling (e.g., 20) there is a good agreement between the computed $\delta^{13}C$ values (-4.1 to $-3.8‰$) and those measured on the emitted CO_2 (-4.3 to $-3.5‰$, [28]), supporting the achievement of chemical and isotopic equilibrium. The above $\delta^{13}C$ range is identical to that found for CO_2 in the high-temperature (800–1090°C) crater exhalations of Etna ($-4.0 \pm 0.5‰$; [13,14]) and in soil gas emanations from its summit (-3.7 to $-4.1‰$, Table 1 and [1]), thus indicating the same carbon source. Being also typical of carbon in C-rich mantle-derived rocks [34], it demonstrates a mantle magma derivation for the dissolved gas.

If one excludes a strong ^3He signal at spring 15 and well 31, located on seismically active faults (Fig. 1), groundwaters outside the above two areas show lower or strictly atmospheric $^3He/^4He$ ratios and are consistently poorer in carbon (Fig. 4a). Their more variable and more negative $\delta^{13}C$ of TDC (-13.0 to $-6.0‰$, Fig. 4b) and CO_2 (down to $-22‰$, Fig. 4c) point to no or a limited magmatic contribution and a prevalently organic derivation for their carbon (decay of organic matter in soils, respiration of plants). Purely organic CO_2 (-36 to $-25‰$) occurs in soil gas and methane-rich bubbles gently rising through water at Fondachello (25, Fig.

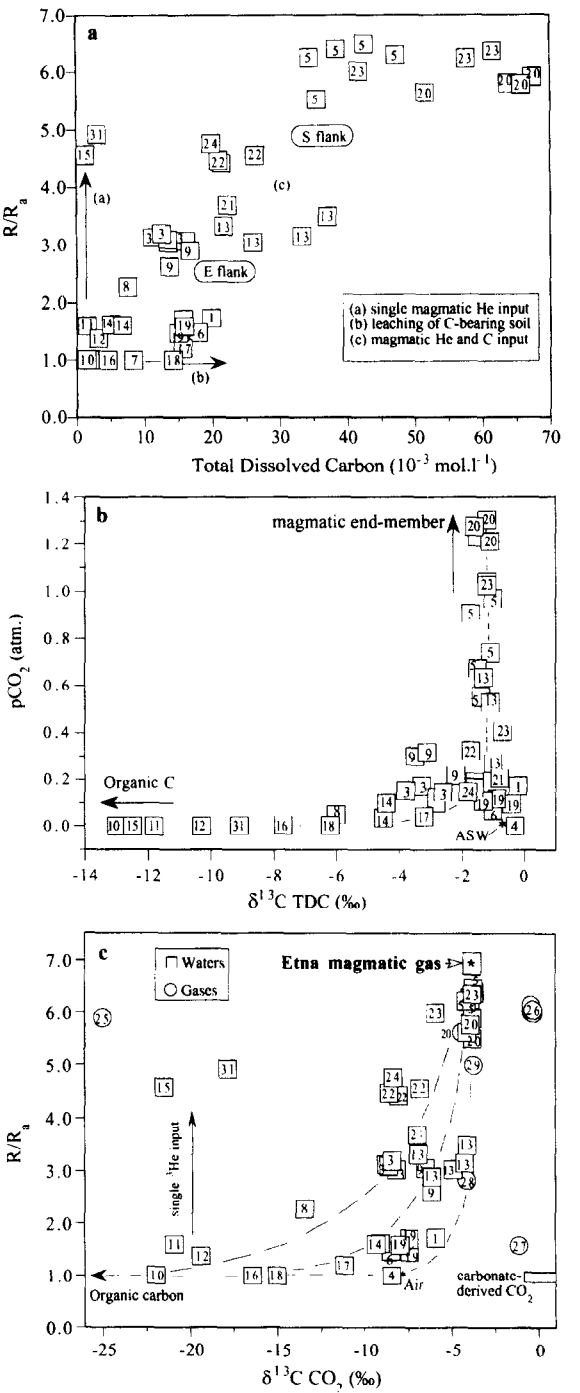

Fig. 4. (a) R/R_a versus total dissolved carbon (TDC) in Etna groundwaters. A preferential, correlated increase in R/R_a and TDC is observed in groundwaters outflowing from the southern and eastern flanks of Etna (see text). Waters poorer in carbon elsewhere have a lower or strictly atmospheric $^3He/^4He$ ratio. An isolated input of ^3He is seen at spring 15 (Pernicana fault, Fig. 1) and well 31. (b) $\delta^{13}C$ of TDC versus pCO_2 in groundwaters. Note the very restricted $\delta^{13}C$ range of TDC (-1.8 to $-1.0‰$) in groundwaters enriched in dissolved carbon, despite wide pCO_2 variation, and the more variable and negative $\delta^{13}C$ for waters depleted in carbon. (c) R/R_a versus $\delta^{13}C$ of CO_2 in groundwaters and gases of Etna. $\delta^{13}C$ values for groundwaters are those computed for CO_2 in isotopic equilibrium with the dissolved carbon species (Table 1). Data for most groundwaters and gases consistently define three-component mixing curves between a ^3He–CO_2-rich magmatic end-member, with $^3He/^4He$ ratio of 6.9 ± 0.2 R_a and $\delta^{13}C$ of about $-4.0‰$, and either the atmosphere or a mixture of dissolved air and organic carbon ($\delta^{13}C \leq -13‰$). See text for discussion.

1), where mud volcanoes were active in the recent past [20,28]. Note, however, that this gas coexists with concentrated helium (478 ppm) whose high $^3He/^4He$ ratio (5.9 R_a) evidences a deep mantle gas leak, partly diluted by crustal He (Fig. 3), occurring along the NE–SW Comiso–Messina tectonic fault which borders the Ionian coast.

In Fig. 4b,c, Etna groundwaters thus define a mixing domain between a He–CO_2-rich magmatic end-member, with R/R_a ratio of 6.9 ± 0.2 and $\delta^{13}C$ of around -4‰, and two He–CO_2-poor surficial components with atmospheric $^3He/^4He$ ratio and lower $\delta^{13}C$, that are either pure dissolved air or a variable mixture of dissolved air and organic carbon. Apart from samples 26 and 27 (the latter being related to residual magma degassing), the gas emanations plot consistently on a mixing trend between the same magmatic end-member and air (Fig. 4c). The curvature of the hyperbolic mixing curves for groundwaters highlights the influence of the higher CO_2/He ratio of the magmatic component. A few waters from either the southern (21, 22 and 24) or the eastern (3, 9 and 13, 04/95) volcano flanks display relatively more negative $\delta^{13}C$ values at constant $^3He/^4He$ ratio and have points somewhat shifted towards the inner side of the hyperbolae. Such a shift may reflect either a greater proportion of organic carbon in the surficial component—for example, in the case of waters 3 and 9, which circulate in contact with sediments (see Section 3.1)—or a chemical and isotopic fractionation of the magma-derived carbon itself during water flow and/or reactions with the host rocks, able to decrease both its C/He ratio and $\delta^{13}C$ (lower hyperbolic curvature). Partial precipitation of calcite during water–rock interactions is one process that could produce such an effect (e.g. in waters 21 and 22, which both include radiogenic He and have a particularly long pathflow, see next section), since $CaCO_3$ concentrates ^{13}C by about 10‰ and 1.8‰ at 20°C at the expense of gaseous CO_2 and bicarbonate, respectively [35]. In contrast, partial CO_2 degassing before outflow could deplete the waters in carbon but not in ^{13}C, because ^{13}C fractionation between gaseous CO_2 and TDC is negative at the temperatures measured [33]. More detailed investigations are currently being undertaken to quantify this aspect.

Finally, the above mixing relationships exclude any widespread contribution of carbon dioxide derived from heated carbonate sediments in the basement. Only the mud pool gases in Paterno (26), which are connected with an ancient eccentric eruptive fracture cutting these sediments, and fumaroles along the 1991–1993 eruptive fracture (#27), which also displayed anomalously high radon activity [36], have a high $\delta^{13}C$ (-1.1 to -0.3‰) compatible with such an origin (Fig. 4b). Nevertheless, ^{13}C fractionation during boiling of a CO_2-rich hydrothermal system (100–150°C), partly fed with magmatic gas, may also account for the high $\delta^{13}C$ of Paterno gases [37]. Hence, these new results suggest that the trend of increasing $\delta^{13}C$ with decreasing CO_2 content that was observed in the volcanic ground of Etna along with the distance from its central conduits [1] more likely results from an isotopic fractionation of magma-derived CO_2 during its deep release and/or subsequent ascent through the volcanic pile than from an increasing leakage of carbonate-derived CO_2 from the basement. This reinforces the idea of an essentially magmatic origin for the gas output from this volcano (see Section 4.2).

3.4. Areas of magmatic gas leaks

Our recognition that groundwaters enriched in both mantle-derived helium and carbon preferentially outflow from two well-defined sectors of the south-southwest and eastern flanks of the volcano provides a new framework for remote monitoring of the interactions between magma degassing and the hydrological system of Etna. The question arises of whether this spatial distribution reflects a localized input of magmatic gas across the two anomalous areas, where CO_2 is also abundant in adjacent soils [20,23,38], or whether it is determined by the hydrological pattern, or both.

As mentioned in Section 3.1 and illustrated in Fig. 5a,b, both magnesium and bicarbonate (but also TDC, pCO_2 and $\delta^{13}CO_2$) tend to increase with the difference in altitude between the recharge and the outflow of groundwaters (Δh, Table 1), with a steeper rate for Δh values ≥ 800 m. In other words, these species are the more enriched because groundwaters originate from a higher elevation on the volcano and/or have a longer pathflow; that is, a deeper infiltration and a longer residence time. In the case

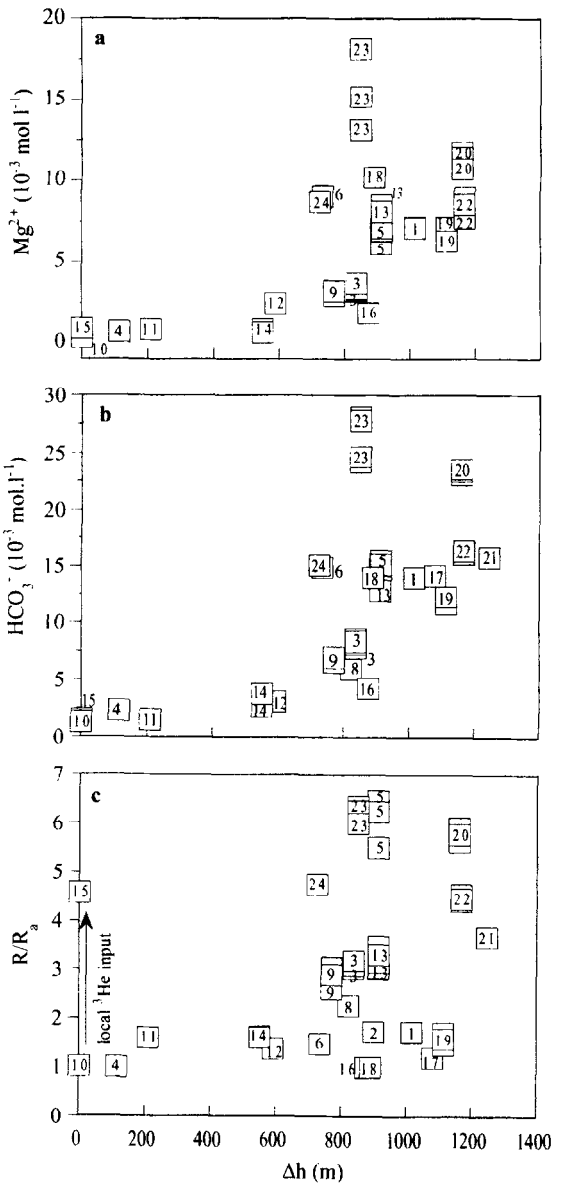

Fig. 5. Variations in Mg, HCO_3^- and $^3He/^4He$ with the pathflow length of groundwaters. (a) Mg vs. Δh. (b) HCO_3^- vs. Δh. (c) R/R_a vs. Δh (see text for discussion).

of magnesium, this trend is consistent with increased leaching of the host basaltic strata. In the case of bicarbonate, however, leaching of the host (previously degassed) basalts is unable to provide the observed amounts of carbon. Rather, the high pCO_2 values require a CO_2-rich gas input into the waters, whose the positive correlation between Mg and HCO_3 provides a measure of the intensity. Accordingly, the increase in HCO_3 with Δh and, in particular, the fact that no water with high bicarbonate occurs at low Δh, point to an input of the CO_2-rich gas through more elevated (more central) parts of the mountain, rather than at the site of water run-off. This conclusion is supported by the observation that, within a given area, waters with a higher outflow elevation tend to have a higher pCO_2 [23]. The coherence between the distribution of points in Fig. 5a,b and the spatial distribution of waters in the field (Fig. 1) also suggests well defined but separate groundwater paths (e.g., the grouping of sites 17, 19, 20, 2, 22, sites 5 and 23 and sites 6 and 24 in the south-southwest anomalous zone). The same conclusions apply to helium, even though the trend for $^3He/^4He$ is less clear-cut (Fig. 5c). Because of the much lower solubility of He than C in water, it is possible that some samples have suffered He degassing and air admixture prior to outflow (e.g., sites 17, 18 and 19 on the south-southwest flank and 1 and 2 on the eastern flank, which display high TDC and Mg but low He and $^3He/^4He$ values). This possibility especially concerns sites 1 and 2, where water is drained within a partially open pipe. Alternatively, some of these waters may have originally contained little magmatic gas, as suggested by their low $\delta^{13}C$ of TDC and CO_2 (Fig. 4c). If one excepts these samples, there is a broad tendency for $^3He/^4He$ to increase like C and Mg along with Δh, suggesting that, instead of a strictly local injection (as at site 15), the magmatic helium in many waters was prevalently solubilized while percolating together with CO_2 through more elevated parts of the volcano.

A privileged area for such a gas stripping is the south-southeast volcanotectonic fracture zone of Etna (Fig. 1), where diffuse release of magma-derived He and CO_2 is the most active [1,36], and along which extensional stress, that would favour the draining and infiltration of rainfall, is sustained by southeastward gravitational spreading of the pile [39]. This deep fracture zone moreover taps a huge plutonic body of basaltic rock, including pockets of molten magma, that extends down to about 10 km beneath Etna [40]. The emergence of gas-charged waters in two remote areas on both sides of this axis is consistent with the hydrogeological conditions [25,27] and would support this idea. It may also help to explain the occur-

rence of quite synchronous increases in pCO_2 in both areas [38], although they are 25 km apart from each other, following shallow dyke emplacement beneath Etna's south-southeastern upper flank a few months prior to the onset of the huge 1991–1993 eruption. These pCO_2 variations have been attributed to a direct input of magmatic gas through local faults in both areas, as a consequence of overpressure in the deep magma feeding system [38]. Both interpretations are not mutually exclusive, however, since overpressure in the deep magma feeding system can be expected to promote an increased gas flux across the deep south-southeast fracture zone of Etna as well. We emphasize here the great potential for underground water flow through the central, gas-effusing parts of the volcano to collect uprising magma-derived volatiles and to transport them quite rapidly towards down-slope areas, where the existence of open faults will subsequently favour hydraulic depressurization, leading to bubbling of the waters. This does not preclude the possibility of a direct gas input through local faults but, if this latter process were dominant, one would expect more independent variations in dissolved gas and magnesium contents in Etnean groundwaters (such as at sites 15, 24 and 31). Further investigations, including the dosing of tritium, which will allow us to constrain the transit time of each water, are needed to settle this point.

4. Discussion

4.1. The mantle source of Etnean volatiles

The inferred R/R_a ratio of ≈ 7 for Etna magmatic gas (and magma) is the highest of any active volcano in continental Europe and supports previous statements made from data on the basalts [2,3]. Together with its $\delta^{13}C$ of $-4.0 \pm 0.5‰$ [1,13,14] and its $CO_2/^3He$ molar ratio of 5.8×10^9 (Table 1), Etna magmatic gas plots at the lower right end of the MORB domain and well outside the field for Hawaiian-type hot spots (Fig. 6). Its $^3He/^4He$ ratio allows a small (13%) addition of radiogenic He to typical MORB material (8 R_a), this may be due to either deep magma–crust interactions [41] or, more plausibly, given the quite steady $^3He/^4He$ range in Etna basalts of different age (including the initial tholeiitic terms [3]) and the non-crustal origin of C and S in the gas [13,14], an enrichment of U–Th and/or ^4He in the magma source itself. An upwelling upper mantle zone, with relatively low Nd and high Sr–Pb isotopic ratios compared to N-MORBs but similar to those in primary Etna basalts, was shown to be a common parent source to volcanism in whole of Western–Central Europe [4]. Therefore, the high, but lower than typical MORB, $^3He/^4He$ ratio at Etna may track this large-scale, but individualized and relatively radiogenic reservoir (in situ ^4He ingrowth; see also [2–4]). The MORB-type $CO_2/^3He$ ratio and $\delta^{13}C$ of Etna gas discard any significant local contamination of this mantle by crustal carbon derived from the nearby subducting African plate margin. In contrast, a northward-increasing imprint of subducted crustal He and C is obvious from volcanoes in the Aeolian arc and Central Italy (Fig. 6), whose the fluids show both a gradual decrease in $^3He/^4He$ and an increase of $\delta^{13}C$ *and* $CO_2/^3He$ [42–44] and whose the magmas are correlatively enriched in K, Rb, U, ^{18}O and ^{87}Sr (e.g. [45,46]). Hence, Etna does not fit with the 'helium boundary', with high ratios within and low ratios outside, that was proposed [42] to run parallel to the Sicilian–Calabrian arc system (Fig. 1): its high $^3He/^4He$ ratio points to its direct feeding, through tensional tectonic faults, by more primary (or less contaminated) mantle underlying the forearc region.

4.2. The Etna degassing budget of mantle C and ^3He

4.2.1. Volatile output

Open-conduit magma degassing through the summit craters of Etna has been estimated to produce $(13 \pm 3) \times 10^6$ t CO_2/yr, on average [1], based on measurements of the SO_2 flux and CO_2/SO_2 ratio in the plume. An output of the same order of magnitude has been estimated for soil flank emanations during periods of fissural lava effusion and/or shallow magma ponding, based on airborne measurements of excess CO_2 in the outside plume downwind atmosphere of the volcano [1]. Recent field investigations [36] suggest a flank emanation rate of about 150–200 and 1000–5000 t/day CO_2/km length of fissure, without and with visible (thermal) emissions, respectively. Thus, a 4 km long degassing fracture,

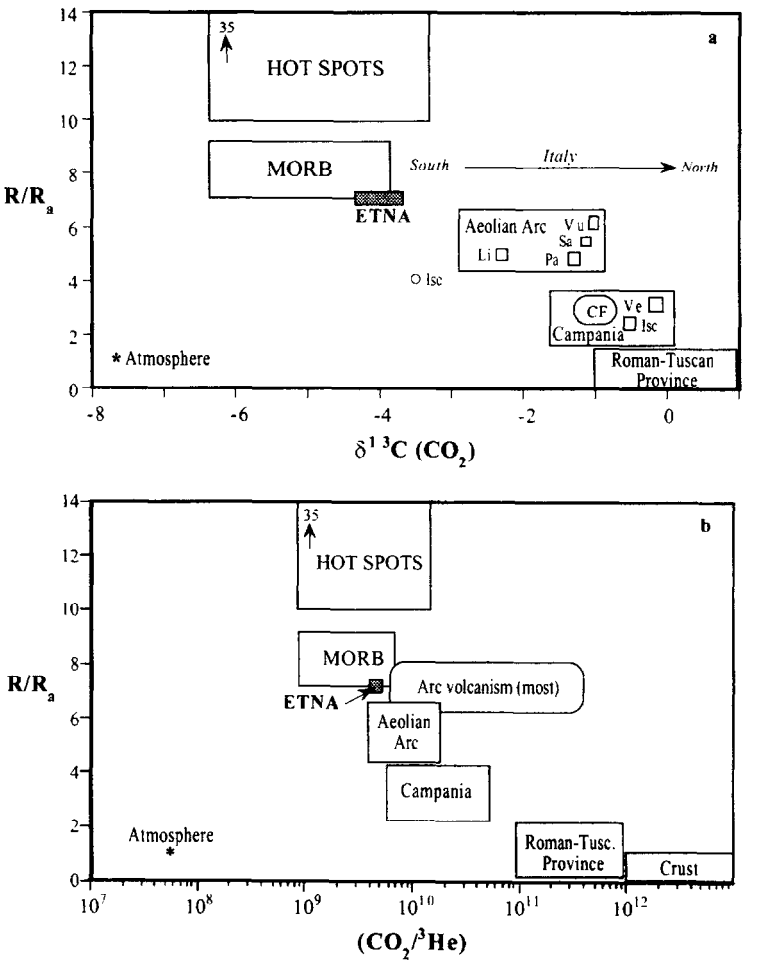

Fig. 6. R/R_a versus (a) $\delta^{13}C$ and (b) $CO_2/^3He$ in fluids from Etna and other volcanoes in Central–Southern Italy. Data for Etna (this work and [1,13,14]) and other Italian volcanoes [42–45] are compared with the respective domains for hot spot and mid-ocean ridge basalts [15,34,51], arc volcanism [51] and continental crust [15,32]. Etna plots to the lower right end of the MORB field, indicating an upper mantle source relatively enriched in radiogenic ^4He [2–4]. Volcanoes further north in the Aeolian Island arc and Southern–Central Italy display a gradual trend of decreasing $^3He/^4He$ and increasing $\delta^{13}C$ and $CO_2/^3He$ towards crustal values, which reflect the influence of regional subduction processes. *Vu* = Vulcano; *Sa* = Salina; *Li* = Lipari; *Pa* = Panarea; *Isch* = Ischia; *CF* = Campi Flegrei; *Ve* = Vesuvius.

such as the ones which fed the 1989 and 1991–1993 eruptions, could emit some $(4–20) \times 10^3$ t/day of CO_2; that is, between 10% and 50% of the mean crater plume output. From the $CO_2/^3He$ ratio of 5.8×10^9 in the magmatic gas (Table 2) one may thus infer a minimal release of 58 ± 13 mole of ^3He per year during both crater and flank degassing at Etna.

The quantity of ^3He and C that is evacuated laterally by groundwaters can be tentatively assessed by combining the mean frequency distribution of dissolved, prevalently magma-derived, carbon in all Etnean waters (about 600 mg/l of TDC as CO_2 [23]), with the estimated groundwater run-off from the volcano (7×10^{11} l/yr, [25]). This yields 0.4×10^6 t/yr of CO_2. This is a minimal figure since important run-off probably occurs below sea water along the Ionian coast [25,27]. Assuming a preserved $CO_2/^3He$ ratio of the magmatic gas during dissolution and transport leads to an output of 1.9 mol/yr of ^3He in the same way. Despite large uncertainties, it appears that underground water flow should carry

only a minor fraction ($\approx 3\%$) of the total Etnean output of mantle-derived He and C. This does not weaken the interest in a survey of these volatiles in sensitive water springs and wells which, in addition, are more easily accessible and measurable than volcanic vents.

4.2.2. Magma degassing budget

The estimated discharge of CO_2 and ^3He by Etna accounts for about 10% and 15%, respectively, of global production of these two species by subaerial volcanism [47,48], further illustrating the exceptional volatile contribution of this alkaline volcano to the atmosphere. A similar proportion has been inferred from its SO_2 output [1]. Such a huge contribution requires that both C and He be abundant in, and efficiently degassed from, the magma. The original content of C and He in Etna alkali basalt is not known but the basalt was found to be oversaturated with pure CO_2 at 700 MPa and 1200°C [9]; that is, at a lithostatic depth corresponding to the subcrustal feeding reservoir of the volcano [5]. Under such conditions a tholeiitic liquid can dissolve 0.65 wt% of CO_2 [49]; the original content of Etna alkali basalt should, therefore, be higher than this. This quantity may be tentatively assessed by relating the original sulphur content of the magma (0.3 wt%, [8–10]) to the C/S ($\approx CO_2/SO_2$) ratio of the volcanic plume and/or the few high-temperature gases sampled from the central craters. This ratio was found to be highly variable, from 3 to 50 by mole [1,14,50], depending on sampling conditions but also on the fact that CO_2 exsolves much earlier than sulphur [8–10] and becomes variably enriched in the gas phase depending on the degree (or depth) of degassing of the magma column [14]. Taking the lower C/S ratio of 3 as more representative of the original undegassed magma (at mantle depth) would lead to an initial CO_2 content of 1.23 wt%, or 2.8×10^{-4} mol/g, corresponding to saturation at $\approx 1.5 \times 10^3$ MPa [49]. As CO_2 and ^3He behave quite similarly during basalt degassing [51], the $CO_2/^3He$ ratio of the gas would then imply an original ^3He content of 4.9×10^{-14} mol/g in the magma, 3 times more than in N-MORBs [15,33,51]. Note that this is consistent with a three-fold enrichment of sulphur in Etna alkali basalt compared to MORBs. When combined with the above flux values, these estimates lead us to compute a magma degassing rate of 0.60 ± 0.14 km^3/yr for both species, about 15 times greater than the mean extrusion rate of basalt over the last two decades (Allard, 1996). We thus conclude that both the CO_2 and ^3He emitted by Etna are essentially derived from deep intrusive degassing of non-erupted magma.

5. Summary

This study has led to the following observations and conclusions:

1. Groundwaters and gas emanations sampled in various sectors of Mount Etna contain ^3He-rich mantle-derived He, variably diluted by air, whose the ultimate $^3He/^4He$ ratio is inferred to be 6.9 ± 0.2 R_a. This component is associated with CO_2 whose the $\delta^{13}C$ ($\approx -4.0‰$) is typical of mantle-derived carbon in high-temperature Etnean exhalations.
2. Both species are preferentially abundant in meteoric groundwaters which outflow from two remote areas of the south-southwest and eastern volcano flanks, with their concentration increasing with the recharge altitude or the pathflow length of the waters. This pattern suggests a prevalent stripping of magmatic gas while groundwaters infiltrate and flow through more elevated, gas-effusing parts of the volcanic pile, among which the south-southeast volcanotectonic fracture zone of Etna is the best candidate. The preferential outflow of ^3He- and CO_2-rich waters in two areas on both sides of this axis provides a favourable framework for remote geochemical monitoring of the volcano.
3. The $^3He/^4He$ ratio of the magmatic gas end-member coincides with that of helium trapped in ^3He-rich olivine crystals of Etnean basalts, thus pointing to its negligible dilution by crustal He. Such a similarity provides an additional constraint on the $^3He/^4He$ ratio of Etna magma, which is the highest of any active volcano in continental Europe. Together with $\delta^{13}C$ and $CO_2/^3He$ data, this ratio suggests that Etna is fed by a relatively radiogenic MORB-type mantle source, which was recognized as the parent source of volcanism in the whole of Western–Central Europe.

4. The output of mantle-derived CO_2 and ^3He from Etna accounts for about 10% and 15%, respectively, of global emissions from subaerial volcanoes. Most of this output is due to persistent open-conduit magma degassing through the summit craters and, to a lesser extent, to diffuse flank emanations. The lateral transport of magmatic volatiles by groundwater flow is of comparatively minor importance. The total Etnean output of CO_2 and ^3He could be sustained by the continuous average degassing of ≈ 0.6 km^3/yr of essentially unerupted magma.

Acknowledgements

This work was supported by the European Community (Environment Programme, contract EV5V-CT92-0177). We acknowledge helpful discussions with J.C. Baubron, B. Marty, T. Trull and M. Valenza and constructive reviews by D. Graham, K. O'Nions and another anonymous referee. ***[MK]***

References

[1] P. Allard, J. Carbonnelle, D. Dajlevic, J. Le Bronec, P. Morel, M.C. Robe, J.M. Maurenas, R. Faivre-Pierret, D. Martin, J.C. Sabroux, P. Zettwoog, Eruptive and diffuse emissions of CO_2 from Mount Etna, Nature 351 (1991) 387–391.

[2] D. Graham, A. Giacobbe, F. Spera, G. Tilton, Chemical and isotopic variations in historical lavas from Mount Etna, EOS Trans. Am. Geophys. Union 73 (1992) 611.

[3] B. Marty, T. Trull, P. Lussiez, I. Basile, J.C. Tanguy, He, Ar, O, Sr and Nd isotope constraints on the origin and evolution of Mount Etna magmatism, Earth Planet. Sci. Lett. 126 (1994) 23–29.

[4] K. Hoernle, Y.S. Zhang, D. Graham, Seismic and geochemical evidence for large-scale mantle upwelling beneath the eastern Atlantic and western and central Europe, Nature 374 (1995) 34–39.

[5] D.K. Chester, A.M. Duncan, J.E. Guest, C.R.J. Kilburn (Eds.), Mount Etna: the Anatomy of a Volcano, Chapman and Hall, London, 1985, 404 pp.

[6] F. Barberi, L. Civetta, P. Gasparini, F. Innocenti, R. Scandone, G. Ferrara, L. Villari, Earth Planet. Sci. Lett. 21 (1974) 269–276.

[7] M. Condomines, J.C. Tanguy, G. Kieffer, C.J. Allègre, Magmatic evolution of a volcano studied by ^{230}Th–^{238}U disequilibrium and trace element systematics: the Etna case, Geochim. Cosmochim. Acta 46 (1982) 1397–1416.

[8] N. Métrich, R. Clocchiatti, Melt inclusion investigation of the volatile behavior in historic alkaline basaltic magmas of Etna, Bull. Volcanol. 51 (1989) 185–198.

[9] R. Clocchiatti, J. Weisz, M. Mosbach, J.C. Tanguy, Coexistence de verres alcalins et tholeiitiques saturés en CO_2 dans les olivines des hyaloclastites d'Aci Castello (Etna, Sicile, Italie). Arguments en faveur d'un manteau anormal et d'un réservoir profond, Acta Vulcanol. 12 (1992) 161–173.

[10] N. Métrich, R. Clocchiatti, M. Mosbach, M. Chaussidon, The 1989–1990 activity of Etna magma mingling and H_2O–Cl–S-rich basaltic magma. Evidence from melt inclusions, J. Volcanol. Geotherm. Res. 59 (1993) 131–144.

[11] J.L. Joron, M. Treuil, Etude géochimique et pétrogenèse des laves de l'Etna, Sicile (Italie), Bull. Volcanol. 47 (1984) 1126–1144.

[12] R. Cristofolini, M.A. Menzies, L. Beccaluva, A. Tindle, Petrological notes on the 1983 lavas from Mount Etna, Sicily, with reference to their REE and Sr–Nd isotope composition, Bull. Volcanol. 49 (1987) 599–607.

[13] P. Allard, The origin of water, carbon, sulfur, nitrogen and rare gases in volcanic exhalations: evidence from isotope geochemistry, in: H. Tazieff and J.C. Sabroux (Eds.), Forecasting Volcanic Events, Elsevier, Amsterdam, 1983, pp. 337–386.

[14] P. Allard, Composition isotopique et origine de l'eau, du carbone et du soufre dans les gaz volcaniques: zones de rift, marges continentales et arcs insulaires, Ph.D. Thesis, Univ. Paris 7, 1986.

[15] J.E. Lupton, Terrestrial inert gases: Isotope tracer studies and clues to primordial components in the mantle, Annu. Rev. Earth Planet. Sci. 11 (1983) 371–414.

[16] Y. Sano, Y. Nakamura, H. Wakita, A. Urabe, T. Tominaga, ^3He emission related to volcanic activity, Science 224 (1984) 150–151.

[17] S.N. Williams, Y. Sano, H. Wakita, Helium-3 emissions from Nevado del Ruiz volcano, Colombia, Geophys. Res. Lett. 14 (1987) 1035–1038.

[18] Y. Sano, Y. Nakamura, K. Notsu, H. Wakita, Temporal variation in helium isotope ratio of hydrothermal system induced by volcanic eruptions, Geochim. Cosmochim. Acta 52 (1988) 1–4.

[19] P. Jean-Baptiste, F. Mantisi, A. Dapoigny, M. Stievenard, Design and performance of a mass spectrometric for measuring helium isotopes in natural waters and for low-level tritium determination by the ^3He ingrowth method, Appl. Radiat. Isotop. 43 (1992) 881–891.

[20] F. Parello, W. D'Alessandro, P. Bonfanti, G. Dongarra, Subsurface gases in selected sites of Mount Etna area, Acta Vulcanol. 7 (1995) 35–42.

[21] W. Rison, H. Craig, Helium isotopes and mantle volatiles in Loihi Seamount and Hawaiian Island basalts and xenoliths, Earth Planet. Sci. Lett. 66 (1983) 407–426.

[22] Y. Sano, H. Wakita, Precise measurements of helium isotopes in terrestrial gases, Bull. Chem. Soc. 61 (1988) 1153–1157.

[23] S. Anza, G. Dongarra, S. Giammanco, V. Gottini, S. Hauser, M. Valenza, Geochimica dei fluidi dell'Etna: le acque sotterranee, Miner. Petrogr. Acta 32 (1989) 231–251.

[24] J.R. Gat, I. Carmi, Evolution of the isotopic composition of atmospheric waters in the Mediterranean sea area, J. Geophys. Res. 75 (1970) 3039–3048.
[25] L. Ogniben, Lineamenti idrogeologici dell'Etna, Riv. Min. Sic. 17 (100–102) 1966, 1–24.
[26] A. Aureli, Idrogeologia del fianco occidentale etneo, in: Proc. 2nd Int. Conf. on Groundwaters, Palermo, Italy, 1973, pp. 425–487.
[27] V. Ferrara, Idrogeologia del versante orientale dell'Etna, in: Proc. 3rd Int. Conf. on Groundwaters, Palermo, Italy, 1975, pp. 91–144.
[28] W. D'Alessandro, S. De Gregorio, G. Dongarra, S. Gurrieri, F. Parello, B. Parisi, Chemical and isotopic characterization of the gases of Mount Etna (Italy), J. Volcanol. Geotherm. Res. (1997), in press.
[29] R.F. Weiss, Solubility of helium and neon in water and seawater, J. Chem. Eng. Data 16 (2) (1971) 235–241.
[30] A.I.E.A. Technical Rep. Ser. 331, Vienna, 1992.
[31] A.M. Duncan, The trachybasaltic volcanics of the Adrano area, Mount Etna, Sicily, Geol. Mag. 115 (4) (1978) 273–285.
[32] P. Morrison, J. Pine, Radiogenic origin of the helium isotopes in rocks, Ann. N.Y. Acad. Sci. 62 (1952) 69–92.
[33] J. Zhang, P.D. Quay, D.O. Wilbur, Carbon isotope fractionation during gas–water exchange and dissolution of CO_2, Geochim. Cosmochim. Acta 59 (1995) 107–114.
[34] T. Trull, S. Nadeau, F. Pineau, M. Polvé, M. Javoy, C–He systematics in hotspot xenoliths: Implications for mantle carbon contents and carbon recycling, Earth Planet. Sci. Lett. 118 (1993) 43–64.
[35] K. Emrich, D.H. Ehalt, J.C. Vogel, Carbon isotope fractionation during the precipitation of calcium carbonate, Earth Planet. Sci. Lett. 8 (1970) 363–371.
[36] J.C. Baubron, Prospection, charactérisation et variabilité temporelle des émanations gazeuses diffuses à l'Etna (Italie): 1993–1994, BRGM Rep. R 38820, 1996, 74 pp.
[37] G. Chiodini, W. D'Alessandro, F. Parello, Geochemistry of gas and waters discharged by the mud volcanoes at Paterno, Mt. Etna (Sicily), Bull. Volcanol. 58 (1) (1996) 51–58.
[38] S. Giammanco, S. Gurrieri, M. Valenza, Soil CO_2 degassing on Mt Etna (Sicily) during the period 1989–1993: discrimination between climatic and volcanic influences, Bull. Volcanol. 57 (1995) 52–60.
[39] A. Borgia, L. Ferrari, G. Pasquare, Importance of gravitational spreading in the tectonic and volcanic evolution of Mount Etna, Nature 357 (1992) 231–235.
[40] A. Hirn, A. Nercessian, M. Sapin, F. Ferrucci, G. Wittlinger, Seimic heterogenity of Mount Etna: structure and activity, Geophys. J. Int. 105 (1991) 139–153.
[41] M. Condomines, J.C. Tanguy, V. Michaud, Magma dynamics at Mt. Etna: constraints from U–Th–Ra–Pb radioactive disequilibria and Sr isotopes in historical lavas, Earth Planet. Sci. Lett. 132 (1995) 25–41.
[42] Y. Sano, H. Wakita, F. Italiano, M. Nuccio, Helium isotopes and tectonics in Southern Italy, Geophys. Res. Lett. 16 (1989) 511–514.
[43] D. Tedesco, P. Allard, Y. Sano, H. Wakita, R. Pece, Helium-3 in subaerial and submarine fumaroles of Campi Flegrei caldera, Italy, Geochim. Cosmochim. Acta 54 (1990) 1105–1116.
[44] D.W. Graham, P. Allard, C.J. Kilburn, F.J. Spera, J.E. Lupton, Helium isotopes in some historical lavas from Mount Vesuvius, J. Volcanol. Geotherm. Res. 58 (1993) 359–366.
[45] K.G. Cox, C.J. Hawkesworth, R.K. O'Nions, J.D. Appleton, Isotopic evidence for the derivation of some Roman Region volcanics from anomalously enriched mantle, Contrib. Mineral. Petrol. 56 (1976) 173–180.
[46] R.J. Ellam, C.J. Hawkesworth, M.A. Menzies, N.W. Rogers, The volcanism of Southern Italy: role of subduction and the relationship between potassic and sodic alkaline magmatism, J. Geophys. Res. 94 (1989) 4589–4601.
[47] S.N. Williams, S.J. Schaeffer, M.L. Calvache, D. Lopez, Global carbon dioxide emission to the atmosphere by volcanoes, Geochim. Cosmochim. Acta 56 (1992) 1765–1770.
[48] P. Allard, Global emissions of helium-3 by subaerial volcanism, Geophys. Res. Lett. 19 (14) (1992) 1478–1481.
[49] V. Pan, J.R. Holloway, R.L. Hervig, The pressure and temperature dependence of carbon dioxide solubility in tholeiitic basalt melts, Geochim. Cosmochim. Acta 55 (1995) 1587–1595.
[50] F. Le Guern, H. Tazieff, C. Vavasseur, P. Zettwoog, Resonance in the gas discharge of the Bocca Nuova, Etna (Italy), 1968–1969, J. Volcanol. Geotherm. Res. 12 (1982) 161–166.
[51] B. Marty, A. Jambon, $C/^3He$ in volatile fluxes from the solid Earth: implications for carbon geodynamics, Earth Planet. Sci. Lett. 83 (1987) 16–26.